Instigating an "identity crisis" to investigate how a *Hox* gene acts in fly legs.

Held, Lewis I., Jr., Andrew L. Davis, and Rachel S. Aybar. Department of Biological Sciences, Texas Tech University, Lubbock, Texas 79409.

The three pairs of legs in *Drosophila melanogaster* have starkly different bristle patterns (Hannah-Alava, 1958). The first leg in particular is easily recognizable by the presence of a unique row of bristles on its basitarsus. This "sex comb" gets its name from (1) its presence only in males, and (2) its resemblance to a hair comb: its bristles are thick, dark, blunt, curved, and aligned in a single file. Hence, the bristles of the sex comb are commonly called "teeth."

The foreleg (in both sexes) also bears a series of evenly-spaced rows of bristles on the anterior face of the tibia and basitarsus (Shroff *et al.*, 2007). These transverse rows ("t-rows") are aligned perpendicular to the proximal-distal axis of the leg, whereas the sex comb runs parallel to it. The t-rows are used for grooming during resting (Szebenyi, 1969; Vandervorst and Ghysen, 1980), while the sex comb is used for grasping during mating (Hurtado-Gonzales *et al.*, 2015). Curiously, the comb arises as an ordinary t-row, but then rotates ~90˚ during the pupal period to assume its final position on the adult leg (Held *et al.*, 2004; Atallah *et al.*, 2009).

How do cells on the foreleg choose fates that differ from those of the simpler midleg, which constitutes an evolutionary ground state (Casares and Mann, 2001)? The foreleg veers away from a midleg fate by expressing the *Hox* "selector" gene *Sex combs reduced* (*Scr*) in precisely those parts of the leg that form the sex combs and t-rows (Barmina and Kopp, 2007; Devi *et al.*, 2012). If *Scr* is disabled, then foreleg cells fail to make either structure and instead act as if they belong to a midleg (Held, 2010; Shroff *et al.*, 2007; Struhl, 1982).

Historically, there have been two schools of thought about how such selector genes function (Castelli-Gair and Akam, 1995; Foronda *et al.*, 2009). The "hierarchical" school postulates that they trigger downstream (effector) genes indirectly via a chain of command, like a cascade of falling dominoes (Doe, 2017; Tsubota *et al.*, 2008). The "micromanager" school asserts that they assign cell states directly in combination with other regulatory factors, like the digits of an area code (Akam, 1998; García-Bellido, 1975).

Operationally, it should be possible to test these models by silencing *Scr* at a late stage. The key question is: do sex comb cells need their *Scr* gene during the final stages of bristle differentiation in order to form a proper row of teeth? The hierarchical model implies that *Scr* should be dispensable since it would have triggered the next gene in the cascade long ago, whereas the micromanager model implies that *Scr* should be needed throughout differentiation.

An experiment of this kind was performed by Tanaka *et al.* (2011). They used the TARGET system (see below) to disable *Scr* in nascent bristle cells and found ~50% fewer teeth but no change in comb rotation or tooth morphology. Their results imply that *Scr* is dispensable for bristle differentiation, though it evidently does play a role in setting tooth number. However, similar experiments by Atallah *et al.* (2014) argue that two other regulatory genes—*Distal-less* (*Dll*) and *dachshund* (*dac*)—are needed for comb rotation and tooth morphology, as well as for tooth number (Randsholt and Santamaria, 2008).

The discrepancy between the role of *Scr* on the one hand and *Dll* and *dac* on the other could be due to a difference in their respective modes of action, but it could be partly illusory, given how the experiments were done. Atallah *et al.* used a different *Gal4* driver from Tanaka *et al.* (see below). In order to rule out artifacts that might be due to this uncontrolled variable, we repeated the Tanaka *et al.* analysis of *Scr* by using the *Gal4* driver employed by Atallah *et al.*

Materials and Methods

Like both Tanaka *et al.* and Atallah *et al.*, we used the "TARGET" (temporal and regional gene expression targeting) procedure (McGuire *et al.*, 2004), which relies on the yeast transgenes *Gal4*, *UAS*, and

Gal80^{ts}. *Gal4* encodes a transcription factor that binds the upstream activating sequence *UAS* (Leung and Waddell, 2004). When *Gal4* is inserted in the *cis*-regulatory region of a given gene—call it *gene A*—then *Gal4* will be expressed at the same time and place as *gene A*, and a desired gene—call it *gene B*—can be turned ON congruently if artificially linked to *UAS*. Tanaka *et al.* used *neuralized*(*neur*)-*Gal4*, but Atallah *et al.* used *scabrous*(*sca*)-*Gal4*.

The distinction between these *Gal4* drivers may seem trivial, but it might explain the difference in outcomes. Both *sca* and *neur* are expressed in bristle precursor cells (Yeh *et al.*, 2000), but *sca* is also expressed in the preceding pool of epidermal cells—the "proneural cluster"—whence precursors are chosen (Renaud and Simpson, 2001; Troost *et al.*, 2015). Thus, we used the same *UAS* as Tanaka *et al.* but the same driver as Atallah *et al.—i.e.*, *sca-Gal4:UAS-dsScrRNAi*. Double-stranded (*ds*) *Scr* RNAi (interfering RNA) stifles transcription of native *Scr*, thus allowing us to assess the effect of disabling *Scr* at a slightly earlier stage than Tanaka *et al.*

The timing of *Gal4* expression is manipulable by the *Gal80^{ts}* component of the system. *Gal80^{ts}* is a temperature-sensitive (*ts*) allele of the yeast's *Gal80* gene, and its transgene is expressed constitutively due to its *tubulin* (*tub*) promoter. At permissive temperature (18°C), Gal80^{ts} protein blocks *Gal4* from activating the gene linked to *UAS*, but at restrictive temperature (30°C) the Gal80^{ts} protein itself becomes nonfunctional. Hence, whatever gene is linked to *UAS* can be artificially turned ON at any desired stage of development by merely shifting developing individuals of the appropriate genotype from an 18°C incubator to a 30°C incubator.

Herein lies another potential problem with how to interpret the data of Tanaka *et al.* They shifted their *tub-Gal80^{ts}*:*neur-Gal4:UAS-ScrRNAi* individuals to 30°C as wandering larvae just before puparium formation (PF), but the ~16 h that appears to be required for full *Gal80^{ts}* inactivation (Pavlopoulos and Akam, 2011) might delay *Scr* knockdown when *neur* turns ON in bristle precursors. Indeed, Atallah *et al.* found that *tub-Gal80^{ts}*:*rotund-Gal4:UAS-[dac or Dll]* larvae had to be shifted ~24 h before PF to attain a maximal effect on sex comb development, though *rotund* (unlike *sca*) is ON throughout the larval period, so this comparison may be moot. Detectable expression of *sca* in the sex comb area begins ~15 h after PF (Atallah *et al.*, 2009).

Given the confounding uncertainties concerning the kinetics of the interacting processes, we decided to document sex-comb effects over a wide span of shift times before (BPF) and after (APF) PF. One obvious virtue of using these post-embryonic shifts (*vs*. *Gal4:UAS* sans *Gal80^{ts}*) is that they bypass any possible complications from *sca* expression during the embryonic period (Mlodzik *et al.*, 1990). Another benefit is that they provide a time line for future investigations.

We crossed *sca-Gal4/CyO; tub-Gal80^{ts}* females with *UAS-ScrRNAi* (on chromosome 3) males and raised the offspring on Ward's *Drosophila* Instant Medium plus live yeast at 18°C.

As a control, we let F_1 offspring complete development at 18°C. For pre-PF shifts we transferred bottles of 3rd-instar F_1 larvae from 18°C to 30°C and collected F_1 pupae every 12 h. For post-PF shifts we maintained the bottles at 18°C, harvested F_1 pupae at 12 h intervals, placed them in humidified petri dishes, and kept them at 18°C until shifting to 30°C. All ages were normalized to 25°C time (Ashburner, 1989). Thus, 12-h (real time) cohorts at 18°C are reported here as 6-h (adjusted) cohorts @25°C due to development being two times slower at 18°C (Held, 1990), while 12-h (real time) cohorts at 30°C are reported as such (development rate≈ rate at 25°C).

In addition to this loss-of-function (LOF) strategy we also conducted a gain-of-function (GOF) experiment where we turned *Scr* ON in *sca*-expressing proneural cells. To that end we crossed *sca-Gal4/CyO; tub-Gal80^{ts}* females with *UAS-ScrWT* (on chromosome 2) males (*WT* denotes the wild-type allele) and raised offspring as before. The F_1 offspring we examined were those with non-Curly wings—namely, *sca-Gal4/+; tub-Gal80^{ts}/UAS-ScrRNAi* males for the LOF analysis (abbreviated *sca>ScrRNAi*) and *sca-Gal4/UAS-ScrWT; tub-Gal80^{ts}/+* males for the GOF analysis (abbreviated *sca>ScrWT*). Curly-winged siblings served as internal controls.

Finally, we crossed *neur-Gal4*, *Kg/TM3*, *Sb* (#6393) males with *UAS-ScrRNAi* (#50662) females to construct *neur>ScrRNAi* F_1 flies (like the ones studied by Tanaka *et al.* but without any *Gal80^{ts}*) so that we could compare the effects of knocking out *Scr* in proneural clusters (*sca-Gal4*) *vs*. disabling it in bristle

precursors alone (*neur-Gal4*). We tried a similar strategy to construct *neur>ScrWT* individuals but were unsuccessful due to poor infertility of the parents.

Nutrition was monitored to avoid overcrowding. Adults were preserved in 70% ethanol. Legs were mounted in Faure's medium (Lee and Gerhart, 1973) between cover glasses and photographed at 200× or 400× magnification with a Nikon compound microscope. Legs were also photographed under a dissecting microscope before mounting, so that the extent of comb rotation could be measured precisely at a consistent viewing angle before any twisting of the legs that often occurs as a result of being sandwiched between cover slips.

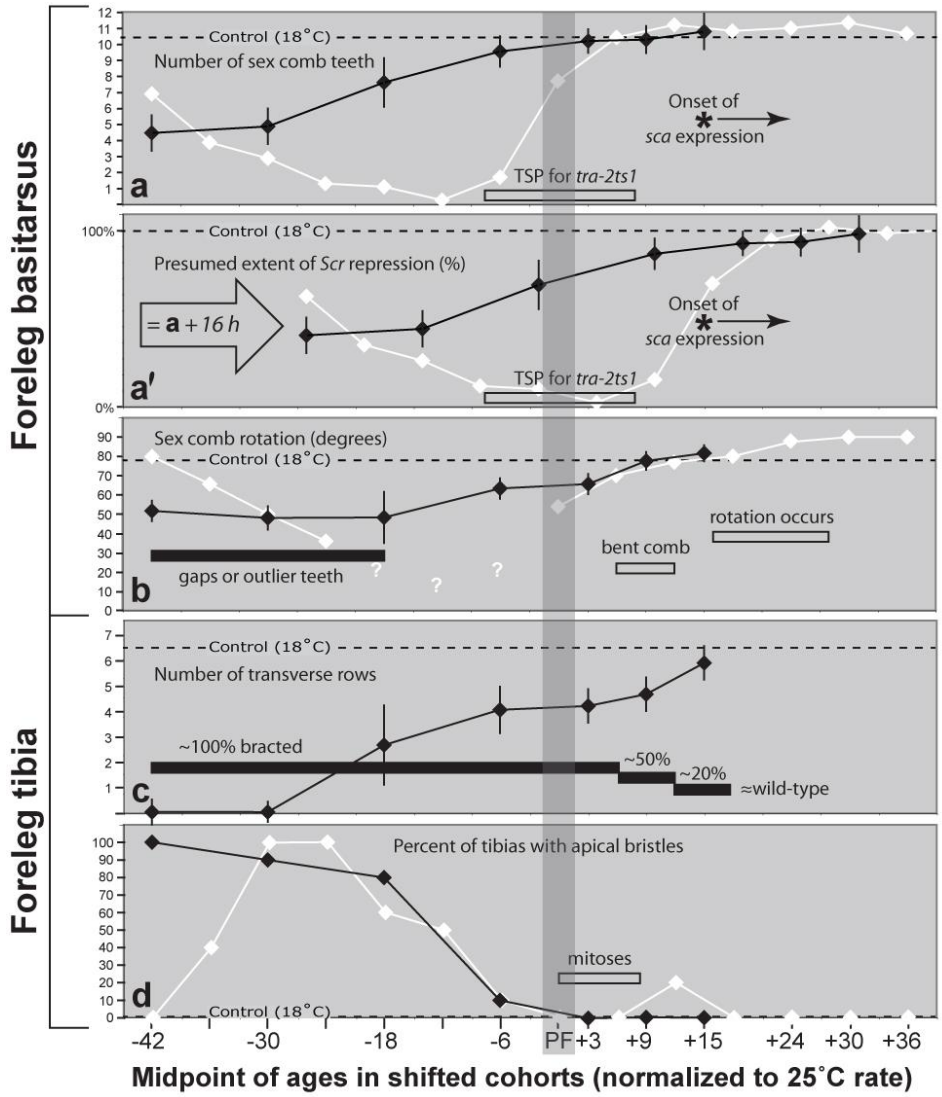

Figure 1 legend, next page.

LOF Analysis: Results and Discussion

Figure 1 summarizes the phenotypes of *Scr*-LOF males. All of these phenotypes constitute partial homeoses from T1 to T2 segmental identity. Like Tanaka *et al.* (2011) we saw ~50% fewer sex comb teeth (Figure 1a) in cohorts shifted before PF, but, unlike them, we observed effects on sex comb rotation (Figures 1b and 2a). This difference is not surprising because the motive force for rotation is generated by nearby cells rather than by the bristle cells themselves (Atallah *et al.*, 2009; Atallah *et al.*, 2014; Malagon and Larsen,

2015). An effect on rotation makes sense for our *sca-Gal4* driver, which is expressed not only in bristle cells (like Tanaka *et al.*'s *neur-Gal4* driver), but also in surrounding epidermal cells within the proneural cluster.

Figure 1. *Scr*-LOF phenotypes caused by transferring cohorts of *sca>ScrRNAi* larvae or pupae from 18°C to 30°C in order to repress *Scr* in proneural clusters. In each panel, data are plotted (y axis) against developmental age at the time of the shift (x axis; normalized to 25°C) relative to puparium formation (PF). Horizontal dashed lines indicate means for control flies raised only at 18°C. Black diamonds denote midpoints of ages when shifted, with vertical lines marking standard deviations. Each point is the mean of 20 legs (= left and right legs of 10 males), unless stated otherwise. Solid bars designate temperature-sensitive periods (TSPs). For comparison, data (white diamonds) are included from a previous *Scr*-LOF experiment (Held, 2010) where pulses—instead of shifts—were used to repress *Scr* throughout the tarsus and distal tibia (via *Dll-Gal4*), and a few other relevant TSPs (open rectangles) are also plotted. **a**. Number of teeth (stout bristles) in the comb. *Asterisk:* earliest time when *sca* expression is detected in the comb area (Atallah *et al.*, 2009). *Open rectangle:* TSP when bristle number is finalized in *transformer2*^{ts1} (*tra2*^{ts1}) sex combs (Belote and Baker, 1982). For *neur>ScrRNAi* flies sans *Gal80*^{ts}, (data not plotted) we saw an average of 4.7 sex comb teeth (s.d. = 0.8, N = 10). **a'**. Data from **a** are re-plotted here, assuming a ~16 h lag until *Gal80*^{ts} is totally disabled after being shifted to 30°C (Atallah *et al.*, 2014; Pavlopoulos and Akam, 2011), though McGuire *et al.* (2004) report a shorter (~ 6 h) lag. Note that the "valley" of *Dll>ScrRNAi* pulses (white diamonds) now coincides with the *tra2*^{ts1} TSP, and the upper "tail" of *sca>ScrRNAi* shifts (black diamonds) now extends beyond the *sca* onset. **b**. Angle of the sex comb relative to transverse axis (perpendicular to proximal-distal leg axis), such that 0° indicates no rotation. N ≈ 20 except for the last three time points, where N = 7, 3 and 5, respectively. Combs of *neur>ScrRNAi* males (data not plotted) rotated normally (~80°; N = 10), as reported previously by Tanaka *et al.* (2011), and 3/10 had gaps or outliers. *Black bar:* TSP for misaligned combs that have a gap or ectopic teeth outside the comb. *Open rectangles:* TSP for bent-comb anomaly (Held, 2010), and period during which the comb rotates in wild-type pupae (Held *et al.*, 2004; Atallah *et al.*, 2009). *N.B.:* Bent-comb TSP was plotted incorrectly in Figure 2b of Held (2010); it is correct here. **c**. Number of t-rows (defined as ≥2 bristle sockets touching transversely) along the proximal-distal axis. Basitarsal t-rows reappeared with a similar time course (data not shown). For *neur>ScrRNAi* males (data not plotted) there was an average of 4.3 t-rows on the tibia (s.d. = 0.9; N = 10) and 4.7 t-rows on the basitarsus (s.d. = 1.8; N = 6), and all tibial t-row bristles were uniformly brown and bracted (as is true for *sca>ScrRNAi*). *Black bars:* Gradual loss of bracts from t-row bristles with later shifts, ultimately reaching the wild-type level where all t-row bristles, except those at the lateral edges, lack bracts. **d**. Extent to which foreleg tibias resemble midleg tibias by the presence of a thick, blunt apical bristle at the distal end of the segment (ventral face). Apical bristles were scored as present even though most were less than half the normal length. Similar effects were observed for *neur>ScrRNAi* males (data not plotted): 70% of male legs (N = 10) had a short apical bristle, while the remainder had none. *Open rectangle:* Time when the precursor of the apical bristle undergoes its two differentiative mitoses (Nottebohm *et al.*, 1994).

In our previous *Dll>ScrRNAi* analysis (Held, 2010) we charted the temperature-sensitive period (TSP) for *Scr*'s role in assigning the number of teeth. That TSP lasts ~2 days @25°C. We used shifts here instead of pulses, so the number would be expected to gradually approach the wild-type level as shifts overlap less and less with this TSP at later times. If we take into account the ~16 h lag of *Gal80*^{ts} inactivation following shifts to 30°C (Pavlopoulos and Akam, 2011), then the "true" TSP would span ~26 h BPF to ~22 h APF (Figure 1a'), instead of ~42 h BPF to ~6 h APF (Figure 1a). With this adjustment, the midpoint of the *Scr*-LOF TSP coincides with a comparable TSP (8 h BPF to 8 h APF) for the sex-determining gene *transformer2* (Belote and Baker, 1982). Given that *sca* turns ON at ~15 h APF (Atallah *et al.*, 2009), enough time should be left in the *Scr*-LOF TSP (~7 h) to permit a partial (~50%) blockage of tooth initiation or maintenance. Based on direct observations of pupal legs (A. Kopp, personal communication), the number of teeth is set by ~15-16 h APF, just before the comb starts to rotate.

This same logic applies to comb rotation, which begins around the time of *sca* activation (Atallah *et al.*, 2009). If *sca>ScrRNAi* is blocking *Scr* at the tail end of its tooth-number TSP, then we might expect disruptions in bristle alignment, since bristle cells merge into a single file around this time (Atallah *et al.*, 2009). Indeed, 8/20, 8/20, and 15/20 legs showed a gap or outlier teeth (Figure 2a) for shifts at 36-48 h, 24-36 h, and 12-24 h BPF, respectively (Figures 1b and 2a). Presumably, the misaligned cells possessed enough Scr to become bristle cells within the proneural cluster, but then suffered a loss of Scr function before they could join together in a chain via homophilic adhesion. Cell adhesion is apparently also impaired on the foreleg tibia because *Scr*-LOF bristle cells fail to form t-rows during this same period (Figures 1c and 2c).

One oddity of the wild-type foreleg is its bracts. Bracts are tiny triangular structures that are induced by bristle cells via the EGFR pathway (del Álamo *et al.*, 2002; Held, 2002b). Most tibial t-rows lack bracts, whereas all basitarsal t-rows possess them (Schubiger *et al.*, 2012). Suppression of *Scr* by *Dll>ScrRNAi* (Held, 2010) or *sca>ScrRNAi* causes virtually all bristles in the t-row area of the foreleg tibia to acquire bracts (Figure 1c), so *Scr* is clearly required for the bractless state of tibial t-rows, and it turns out to be sufficient as well, because overexpressing *Scr* via *Dll>ScrWT* (Held, 2010) or *sca>ScrWT* (see GOF Analysis) deletes bracts from all six legs. Another oddity of tibial *vs*. basitarsal t-rows in wild-type flies is that tibial bristles are yellow, while basitarsal ones are brownish like most other leg bristles (except sex comb teeth, which are black). Among the *Scr*-LOF flies, all t-row bristles were brown, regardless of shift time—indicating the necessity of *Scr* for yellow coloration and suggesting that the TSP for color assignment lies outside the range of ages examined (*i.e*., beyond 15 h APF).

The contemporaneous need for *Scr* gene function when tooth identity, comb rotation, and cell alignment occur is consistent with analogous findings of a need for *Ubx* when midleg-specific traits—sternopleural bristles and the tibial apical bristle—are suppressed during the final stages of bristle differentiation on the hindleg (Rozowski and Akam, 2002). Both of these *Hox* genes appear to be behaving more like intrusive micromanagers than as aloof executives.

Our suppression of *Scr* activity in foreleg proneural cells is evidently causing them to adopt a midleg identity at the very time that they are executing their foreleg-specific instructions. In order to see whether midleg-specific traits can be evoked at such a late stage, we examined foreleg tibias for the presence of the apical macrochaete that is normally only found on midlegs (Hanna-Alava, 1958). Indeed, 20/20, 18/20, and 16/20 forelegs showed an enlarged, thick, blunt bristle at the apical site for shifts at 36-48 h, 24-36 h, and 12-24 h BPF (Figure 1d). However, these bristles never attained more than half the length of a midleg apical bristle (Figure 3), and side-by-side duplicate bristles were common (6/20, 3/20, and 4/20, respectively)—implying that several cells in the proneural cluster start to become apical bristles but then fail to compete by lateral inhibition (Castro *et al.*, 2005) so as to yield a single "victor" whose rival cell regresses back to an epidermal state.

Mechanistically, our conclusion about *Hox* genes acting as micromanagers implies that Hox proteins bind the *cis*-enhancers of effector genes when bristle identity is being implemented (Pavlopoulos and Akam, 2011). If so, then the targeted *cis*-regulatory regions would resemble a rugby scrum where transcription factors from all levels of the control hierarchy area converge simultaneously. Other suspected regulators inside this "huddle", aside from Scr, include Dsx-M, Dac, and Dll (Atallah *et al.*, 2014; Kopp, 2011; Tanaka *et al.*, 2011).

The main exception to this rule of combinatorial action, as Tanaka *et al.* have noted, is bristle shape. Once *Scr* licenses the decision of a bristle precursor to be (or not to be) a sex comb tooth, it evidently delegates the implementation of the tooth's unique shape to subsidiary genes, since no intermediate morphologies were found in the present *Scr*-LOF/GOF study nor in our previous one (Held, 2010), regardless of the time of the shift or pulse. Indeed, the TSP for altering bristle shape—as ascertained using *transformer2*—appears to occur just after the TSP for tooth number (Belote and Baker, 1982). Although sex-determining genes like *tra2* and *dsx* may act directly in assigning bristle shapes (Tanaka *et al.*, 2011; *cf*., Atallah *et al.*, 2014), *Scr* apparently does not.

GOF Analysis: Results and Discussion

We employed the same *UAS-ScrWT* construct (#7302) from the Bloomington Stock Center (*WT* = wild-type allele) that we had previously used with a *Dll-Gal4* (*Distal-less-Gal4*) driver (Held, 2010). In that case, *Dll-Gal4* drove *ScrWT* expression throughout the epidermis of the distal tibia and tarsus, starting at either 20 h or 12 h BPF (when we shifted flies to 30°C). Under those conditions *Scr*-GOF caused ectopic sex combs and t-rows on all six legs, plus yellow bristle pigmentation and pervasive loss of bracts. Curiously, the extra t-rows occurred not only on the anterior surface of midlegs and hindlegs—as would be expected from *Scr*'s role on forelegs—but also on the posterior surface of midlegs (Figure 4d). Some extra t-rows were also found on the posterior side of the foreleg, but to a much more limited extent, as discussed below.

Milder versions of those same *Dll>ScrWT* effects were observed here with *sca>ScrWT*, except for yellowish pigmentation, which might require earlier or longer expression of *ScrWT* than available with *sca-Gal4*. Because our *Scr*-GOF effects were so subtle, we focused on flies that had maximal phenotypes—namely, those from the earliest age we shifted (36-48 h BPF). No experimental (non-Curly) flies survived to eclosion, so we had to dissect pharate adults out of their pupal cases to study them. The anatomical features of those flies will now be described.

Ectopic teeth were only found on forelegs (not on midlegs or hindlegs as in *Dll>ScrWT*): either one (17/20 legs) or two (3/20 legs) isolated teeth were present on the 2nd tarsal segment, and 15/20 forelegs also had a tooth on the 3rd (3/20 cases) or 4th (9/20 cases) tarsal segment or on both of them (3/20 cases) at locations homologous to the sex comb site on the basitarsus. This tendency for extra teeth to arise at these tarsal locations is attributable to regulatory genes other than *Scr* (Barmina and Kopp, 2007; Randsholt and Santamaria, 2008; Tanaka *et al.*, 2011).

The foreleg tibias of control flies (raised at 18°C) contained an average of 6.6 t-rows on their anterior face (s.d. = 0.5; N = 20) like wild-type flies. In contrast, the t-row area on foreleg tibias of shifted (*sca>ScrWT*) flies expanded proximally to reach twice that number in some cases (max. = 13; mean = 9.8; s.d. = 1.7; N = 20; Figure 5a). Strangely, we found a similar, albeit weaker, effect on the posterior side of the hindleg tibia (Figure 5c), which canonically has a single row (Figure 5d), but in *sca>ScrWT* flies had an average of 3.0 rows (s.d. = 1.1; N = 20). The extra rows had as few as two bristles each but arose at intervals typical of foreleg t-rows.

The hindleg is governed by *Ubx*, so *Scr* and *Ubx* could be cooperating synergistically there. This notion finds support in the dramatic effects of *Dll>ScrWT* on hindleg tibias (Figure 8a), where the number of posterior t-row bristles skyrockets four-fold or six-fold from a mean of 8 (wild-type) to a mean of 34 (shift = 20 h BPF) or 47 (shift = 12 h BPF). For some reason the excess t-rows are more irregular on hindlegs than on forelegs (Figure 5e).

Ectopic t-rows that are caused by *sca>ScrWT* (on all six legs) usually consist of only a few adjacent bristles each, instead of the much broader t-rows seen in *Dll>ScrWT* flies (Figure 4). On *sca>ScrWT* forelegs, such minimal—or "incipient"—t-rows were detectable on the posterior face of the tibia and basitarsus, while on hindlegs, they were visible on the anterior face (Figure 6). Comparable ectopic t-rows have been reported for midleg and hindleg basitarsi when *ScrWT* is expressed via a *rotund(rn)-Gal4* driver (Shroff *et al.*, 2007), but it is unclear whether the t-rows in that case arose on both faces of *rn>ScrWT* midlegs or only on the anterior side (T. Orenic, personal communication).

Midlegs offer an ideal opportunity to test the idea that *Scr* fosters t-row formation both anteriorly and posteriorly, because they manifest no t-rows whatsoever in wild-type flies (Figure 7) and hence provide a "blank slate" baseline. Hence, we tallied extra bristles between longitudinal rows ("l-rows") 7 and 8 (anterior face) and between l-rows 1 and 2 (posterior face)—recording only those bristles whose sockets were (1) transversely aligned with a socket of an l-row bristle and (2) physically touching that socket. In a sample of 20 midleg basitarsi, there was a mean of 4.25 thusly defined t-row bristles on the anterior side (s.d. = 2.07) and a mean of 4.60 such bristles on the posterior side (s.d. = 1.43). These averages do not differ significantly ($p > 0.05$; t-test), and thus are consistent with the symmetry hypothesis. Interestingly, *Ubx*-GOF can also induce t-rows on midlegs like *Scr*-GOF (Shroff *et al.*, 2007), but we do not yet know whether it induces them symmetrically on both sides of the leg (T. Orenic, personal communication).

This ability of *sca>ScrWT* to evoke partial t-rows equally on both faces of the midleg suggests that *Scr* function is not being inhibited by *engrailed* (*en*)—a selector gene for the posterior compartment in all legs (*cf*., Held, 2002a). On the other hand, the relative inability of *Dll>ScrWT* to elicit more than a few t-rows on the posterior face of the foreleg (Figure 4b) implies that *en* is preventing *Scr* from inducing t-rows there. This paradox prompted us to go back and comprehensively measure the extent to which extra t-rows are induced on the anterior (A) *vs*. posterior (P) faces of forelegs, midlegs, and hindlegs by *Dll>ScrWT* (vis-à-vis *sca>ScrWT*).

Figure 2. Effect of *sca>ScrRNAi* (*Scr*-LOF) on the foreleg basitarsus (**a**, **b**) and tibia (**c**, **d**). All images are from right legs, oriented with proximal-distal from top to bottom (transverse axis runs perpendicularly) and ventral to the right, at the same scale (bar = 100 microns). **a**. Basitarsus (anterior view) from a *sca>ScrRNAi* male shifted to 30°C at ~42 h BPF (cohort: 36-48 h BPF). There are six teeth, five of which occupy a single file (lower arrowhead) oriented at 52° to the transverse axis. The sixth tooth (upper arrowhead) is an outlier that might have migrated on its own, but it could instead have arisen *in situ* since it belongs to the most distal t-row—a common anomaly in artificially selected strains (N. Malagon, personal communication). Anteroventral bristles (right half of this image), which would normally form t-rows, are fewer and less aligned, with no bristle sockets in contact. The reduction in tooth number and absence of t-rows reflect homeosis. **b**. Basitarsus (anteroventral view) from a control *sca>ScrRNAi* male raised entirely at 18°C (wild-type phenotype). The sex comb has 12 teeth, all of which occupy a single file, and the comb has rotated to ~80°. Seven t-rows are visible in the upper part of the segment, where the sockets of adjacent bristles are nearly all in contact. The dark triangular structures above the bristle sockets are bracts. **c**. Tibia (anterior view) from a *sca>ScrRNAi* male shifted to 30°C at ~42 h BPF (cohort: 36-48 h BPF). The macrochaete (lower left) is the pre-apical bristle (pAB), whose thickness is typical of a midleg. The apical bristle is out of focus on the opposite side of the segment. Note the absence of t-rows, the ubiquity of bracts (except on pAB), and the sparseness of bristles compared to t-row area in **d**. **d**. Tibia (anterior view) from a control *sca>ScrRNAi* male raised entirely at 18°C (wild-type phenotype). T-rows of lighter colored bristles decorate the anteroventral face. The central bristles within each t-row lack bracts; the same is true for the solitary t-row at the distal tip of the hindleg tibia (Figure 5d). The pAB (out of focus) is thinner than the pAB in **b**—another indication, albeit subtler than the apical bristle (Figure 3b), that the *Scr*-LOF leg in **b** has undergone a partial T1-to-T2 homeosis.

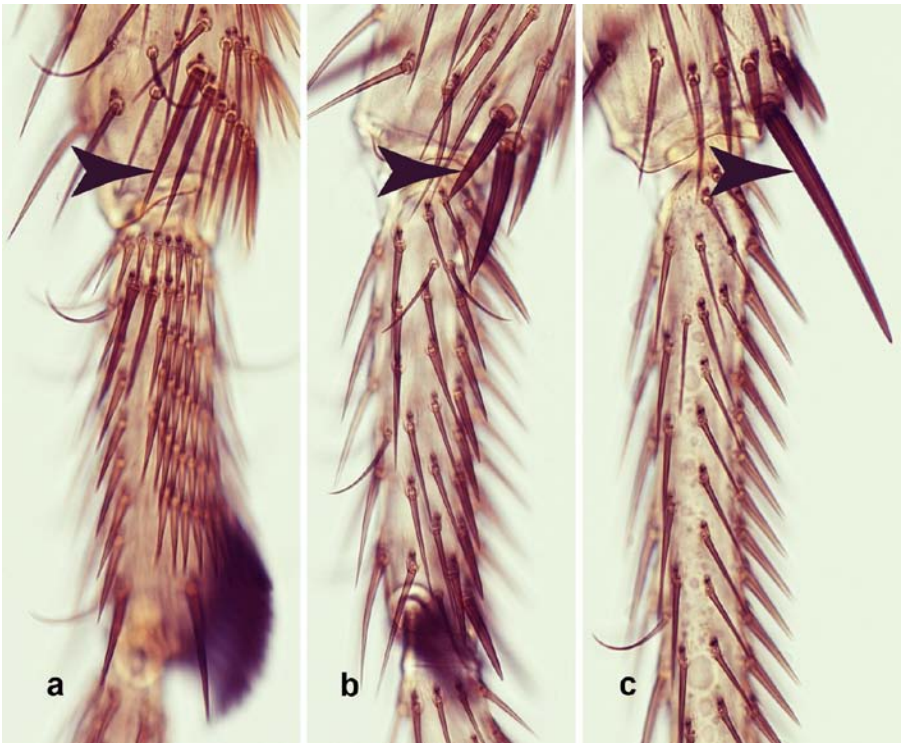

Figure 3. Homeotic production of one or more midleg-like apical bristles on the *sca>ScrRNAi* (*Scr*-LOF) foreleg tibia. All images are at the same scale. **a**. Distal tip of the left foreleg tibia and basitarsus (ventral view) from a control *sca>ScrRNAi* male raised at 18°C (wild-type phenotype). Arrowhead indicates the distalmost t-row, whose two most lateral bristles are characteristically larger and darker than other t-row bristles. **b**. Distal tip of the left foreleg tibia and basitarsus (posterior view) from a *sca>ScrRNAi* male shifted to 30°C at ~42 h BPF (cohort: 36-48 h BPF). T-rows are absent. In place of the last t-row are two bristles (arrowhead), both of which resemble a midleg apical bristle in thickness and pigmentation, but neither attains full length. These bristles could be transformed versions of the dark bristles denoted in **a** (based on unpublished data supplied by M. Rozowski, personal communication), though they reside more distally (see text for an alternative idea). **c**. Distal tip of the right midleg tibia and proximal three-fourths of the basitarsus (posterior view) from a control *sca>ScrRNAi* male raised entirely at 18°C. (The original image was flipped left-right here for ease of comparison.) Arrowhead points to the apical macrochaete. It is crowned by an arc of stout, dark spur bristles (Hannah-Alava, 1958) that are aligned like a foreleg t-row but lacking socket-to-socket contact.

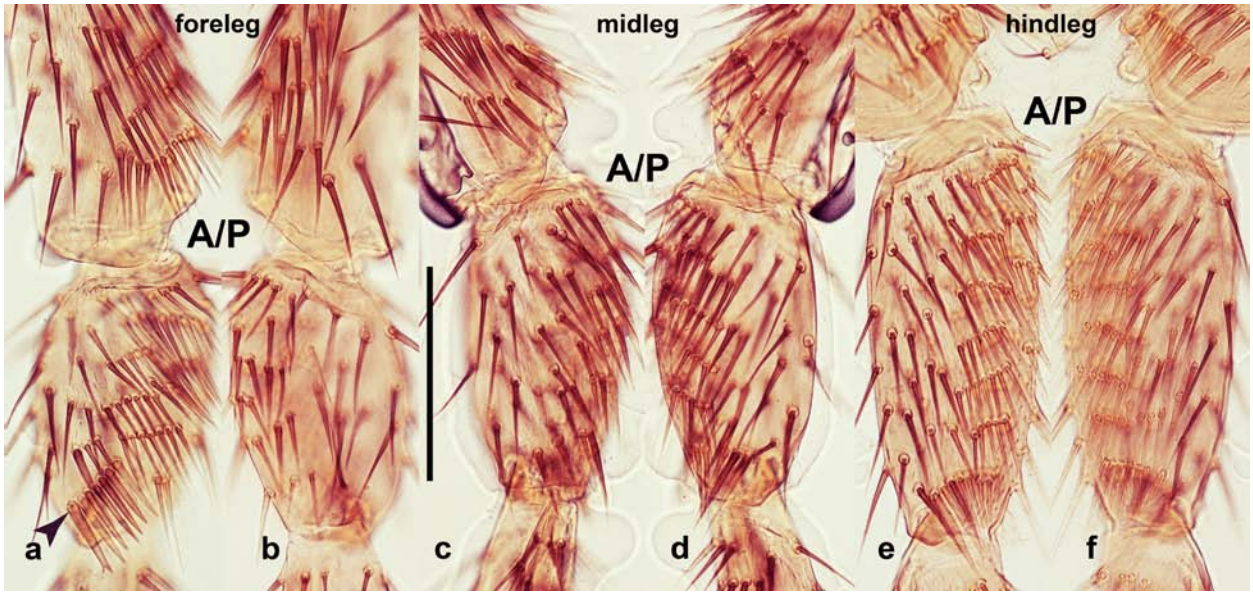

Fiigure 4 (legend on next page).

Figure 4 (previous page). Extra t-rows induced by *Dll>ScrWT* (*Scr*-GOF) on a foreleg (**a**, **b**), a midleg (**c**, **d**), and a hindleg (**e**, **f**). These specimens are from a previous study (Held, 2010), and they are depicted here to facilitate comparison with the similar—but milder—effects of *sca>ScrWT*. They are representative examples of phenotypes seen when *Dll-Gal4/UAS-ScrWT; tub-Gal80ts/+* larvae are shifted to 30°C at 12 h BPF. All photos are at the same magnification, but images for the (left) midleg and hindleg were flipped left-right so as to match the (right) foreleg. Bar length = 100 microns. Leg segments are shorter and wider than the wild type (*cf*., Figure 2b), and bristles are yellower and bractless. Segments are viewed from anterior (A) or posterior (P). **a**, **b**. "Mug shots" of A (**a**) and P (**b**) surfaces of the distal tibia and basitarsus from a foreleg. Note the partly rotated sex comb (arrowhead) and the single outlier tooth on the A side, and the sparsity of ectopic t-rows on the P side of the tibia and basitarsus. **c**, **d**. A (**c**) and P (**d**) surfaces of the distal tibia and basitarsus from a midleg. Note the roughly equal numbers of ectopic t-rows on both faces. (Brown arc at edge is a bubble.) **e**, **f**. A (**e**) and P (**f**) surfaces of the distal tibia and basitarsus from a hindleg. The number of t-rows is roughly symmetric. The t-rows are wide, but they fail to encircle the circumference. Why? Probably because *Scr* is repressed by Dpp (T. Orenic, personal communication). Dpp diffuses from the dorsal midline (Held, 2002a), and if the Dpp gradient has a fixed slope, then its inhibition of *Scr* might explain why the wild-type t-row area is triangular on the (conical) tibia, but rectangular on the (cylindrical) basitarsus.

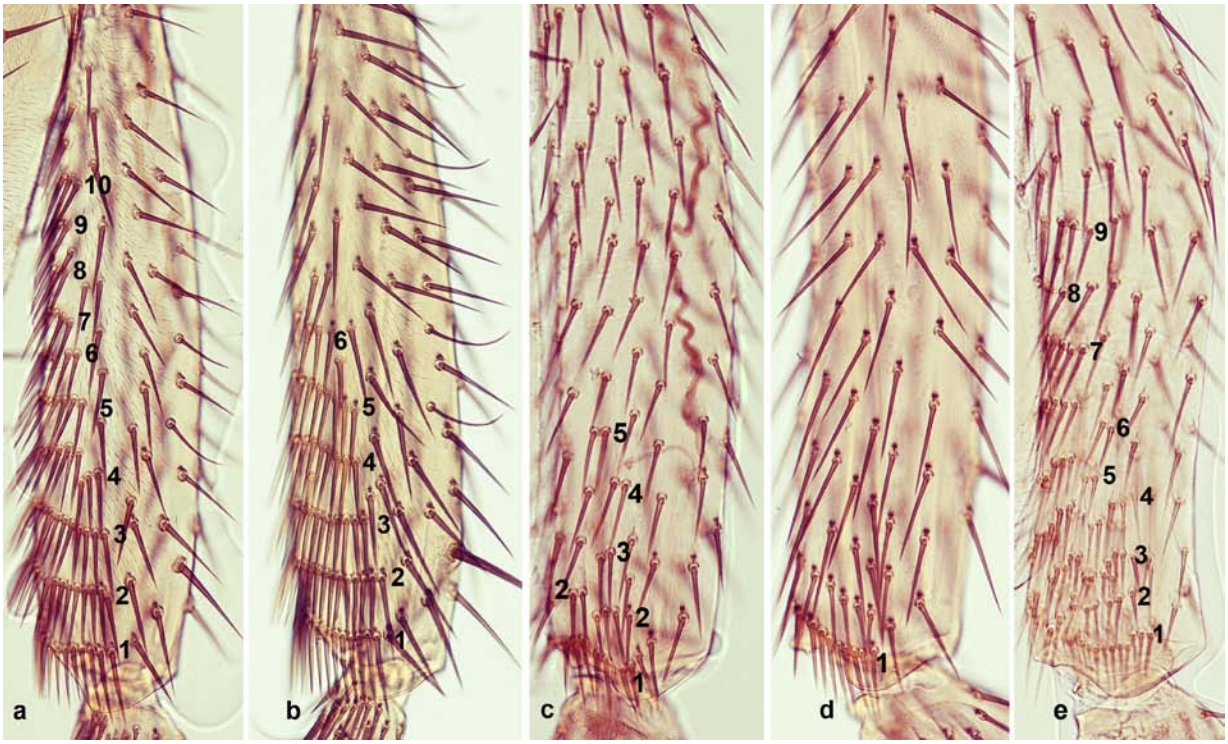

Figure 5. Effects of *Scr*-GOF on t-rows of the foreleg and hindleg tibias. All images are at the same magnification. **a**. Left foreleg tibia (anterior view, ventral to the left) from a *sca>ScrWT* male shifted to 30°C at ~42 h BPF (cohort: 36-48 h BPF). T-rows are numbered from the distal end. Four extra t-rows (#7-10) are visible relative to the control tibia (**b**), presumably due to the extra dosage of Scr in the t-row region (*cf.*, Shroff *et al.*, 2007). The maximum we saw in any specimen was a total of 13 t-rows. Extra rows also develop on foreleg tibias of *Dll>ScrWT* flies (Held, 2010). **b**. Left foreleg tibia (anterior view) from a

Figure 5 (continued). control *sca>ScrWT* male raised entirely at 18°C (wild-type phenotype). Control tibias typically have 6 (as here) or 7 t-rows. Most tibial t-row bristles lack bracts (except at lateral termini)—unlike basitarsal t-row bristles (Figure 2b)—and they are yellower. In contrast, *Sca*-GOF tibial t-row bristles (**a**) are browner, like the surrounding non-t-row bristles. **c**. Right hindleg tibia (posterior view, ventral to the left) from a *sca>ScrWT* male shifted to 30°C at ~42 h BPF (cohort: 36-48 h BPF). T-rows are numbered from the distal end. Four extra, albeit tiny, t-rows (#2-5) are visible (an extreme case) relative to the control tibia (**d**), presumably due to the extra dosage of Scr in the t-row region (*cf*., Shroff *et al.*, 2007). The second t-row has a gap, and rows #3-5 contain only two bristles each. Most bristles lack bracts, unlike the control tibia (**d**). **d**. Right hindleg tibia (posterior view, ventral to the left) from a control *sca>ScrWT* male raised entirely at 18°C (wild-type phenotype). Control tibias have only one t-row (as shown here) containing an average of 8.1 bristles (N = 20). The central bristles of that row consistently lack bracts—like the t-rows on the foreleg tibia (**b**). **e**. Right hindleg tibia (posterior view, ventral to the left) from a *Dll>ScrWT* male shifted to 30°C at 12 h BPF. This profusion of t-rows may stem from a synergy between endogenous *Ubx* and ectopic *Scr* (see text). Numbering of t-rows is approximate because of their many irregularities. The yellow color of bristles in the distal half of the tibia (**e**) is attributable to a longer exposure to *Scr* in the *Dll* region than that afforded by *sca-Gal4* (**c**), but bracts are missing in both cases.

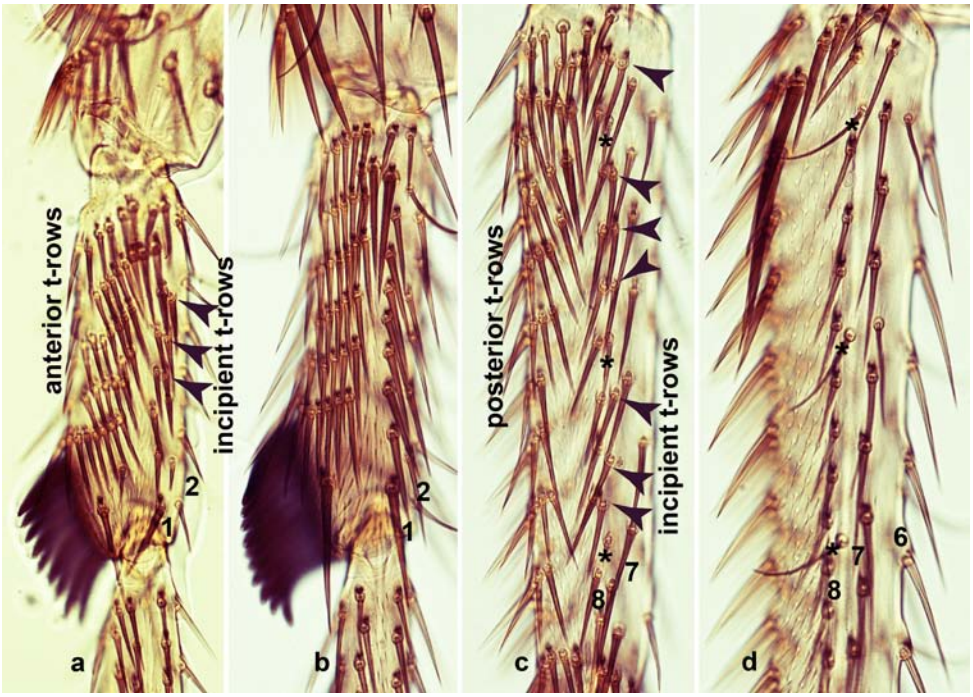

Figure 6. Induction of incipient ectopic t-rows on foreleg and hindleg basitarsi of *sca>ScrWT* (*Scr*-GOF) flies. All photos are at the same magnification. **a**. Right foreleg basitarsus (ventral view) from a *sca>ScrWT* male shifted to 30°C at ~42 h BPF (cohort: 36-48 h BPF). Arrowheads indicate 3 extra bristles between l-rows 1 and 2 (numbered below), which meet the criteria of t-rows (≥2 bristle sockets touching transversely). Evocation of t-rows by *Scr*-GOF on the posterior side challenges the traditional view that *Scr*'s presumed role is to serve as an anterior-specific t-row selector gene (Shroff *et al.*, 2007). **b**. Right foreleg basitarsus (ventral view) from a control *sca>ScrWT* male raised entirely at 18°C (wild-type phenotype). Note the lack of bristles in the narrow corridor between l-rows 1 and 2, except for one chemosensory (curved) bristle near the proximal end. **c**. Left hindleg basitarsus (ventral view) from a *sca>ScrWT* male shifted to 30°C at ~42 h BPF (cohort: 36-48 h BPF). Arrowheads indicate 7 extra bristles between l-rows 7 and 8 (numbered below), which meet the criteria of t-rows. Asterisks label the shafts of

Figure 6 (continued). chemosensory bristles that are recognizable by socket shape, shaft curvature, and thin shaft at base (Held, 2002a). In wild-type legs (**d**) such bristles lack a bract, but *Scr*-GOF deletes many bracts, thus precluding identification here based on that feature alone. Curiously, two of the asterisked bristles appear to be forming incipient t-rows, even though such bristles don't normally abut l-row bristles in wild-type flies (**d**). **d**. Left hindleg basitarsus (ventral view) from a control *sca>ScrWT* male raised at 18°C. Note the absence of bristles in the corridor between l-rows 7 and 8, except for three chemosensory bristles (asterisks) near row 8.

Figure 7. Induction of incipient ectopic t-rows on midleg basitarsi of *sca>ScrWT* (*Scr*-GOF) flies. This slight T2-to-T1 homeosis is trivial compared with the massive eruption of t-rows on *Dll>ScrWT* midlegs (Figure 4)—attributable to a shorter duration of *ScrWT* action from *sca-Gal4*. **a**, **b**. "Mug shots" of right foreleg basitarsus from a *sca>ScrWT* male shifted to 30°C at ~42 h BPF (cohort: 36-48 h BPF), as seen from the anterior (**a**) or posterior (**b**). **a**. Arrowheads indicate five extra bristles between l-rows 7 and 8 (numbered below), which meet the criteria of t-rows (≥2 bristle sockets touching transversely). Most of the extra bristles abut row-8 bristles, but rarely (*e.g.*, lowest arrowhead) they abut a bristle in row 7. **b**. Arrowheads denote four extra bristles between rows 1 and 2 (numbered below), which meet the criteria of t-rows. Three of the extra bristles (first, second, and fourth counting from proximal end) are also aligned with (though not touching) a bristle in row 2. Many basitarsal bristles are missing bracts—another effect of *Scr*-GOF (see text). **c**, **d**. Right foreleg basitarsus from a control *sca>ScrWT* male raised at 18°C (wild-type phenotype). There are no adventitious bristles between l-rows. Curved (bractless) bristles are chemosensory (Held, 2002a).

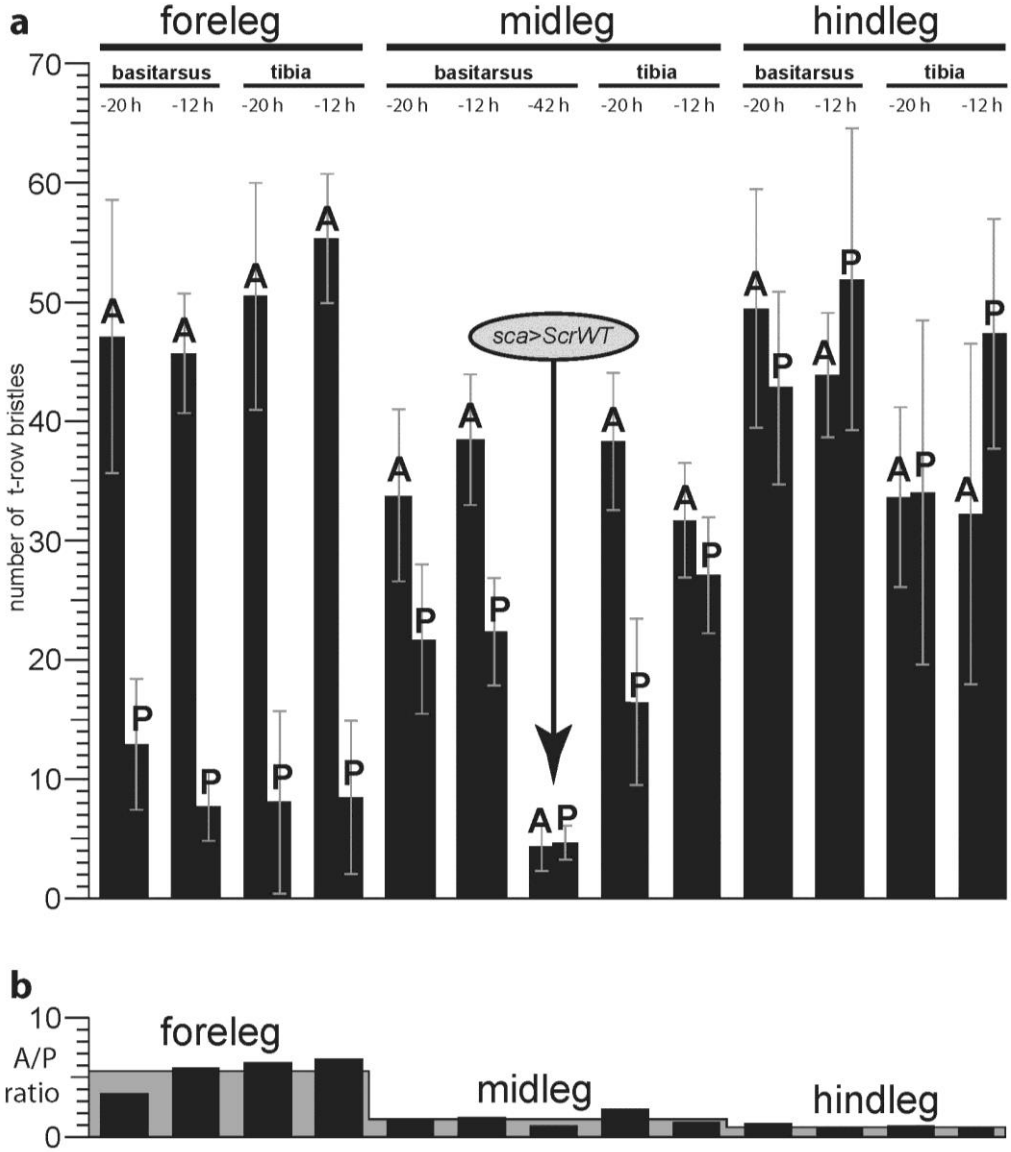

Figure 8. Quantitative analysis of *sca>ScrWT* (present study) *vs*. *Dll>ScrWT* (Held, 2010) with regard to the number of t-row bristles on anterior (A) and posterior (P) faces of forelegs, midlegs, and hindlegs. **a**. Average numbers of t-row bristles (error bars = standard deviations) plotted on the y axis for A and P faces of basitarsi and tibias from *Dll>ScrWT* flies (N = 8 legs/histogram bar) shifted to 30°C at 20 or 12 h BPF, plus a center pair of histograms for *sca>ScrWT* flies (N = 20 legs/histogram bar) shifted to 30°C at ~42 h BPF (cohort: 36-48 h BPF). Mean number of t-row bristles in controls (≈ wild-type) is 42.3 for foreleg basitarsus (N = 10), 64.3 for foreleg tibia (N = 10), and 8.6 for hindleg tibia (N = 10), which contains only a single row. Note the 4- or 6-fold increase in bristle number for the P side of hindleg tibia (20 or 12 h BPF, respectively) above the control level (8.6). **b**. A/P ratios (y axis) computed from the average numbers of t-row bristles on A *vs*. P faces of basitarsi and tibias plotted in histograms above (**a**). The averages of these ratios for forelegs, midlegs, and hindlegs are plotted as gray rectangles.

Figure 9. *Scr*-GOF (*sca>ScrWT*) pharate adult male (**a**) compared to a control (*Curly*-balancer) male sibling (**b**), both of which were shifted from 18°C to 30°C at ~42 h BPF (cohort: 36-48 h BPF). **a**. Most head and thoracic macrochaetes are missing, though tiny bristles do remain at a few sites. Thoracic microchaetes are relatively unaffected. Abdominal bristles are appreciably smaller. **b**. This control fly had partly eclosed from its pupal case when it died, so its body is longer than that of the *sca>ScrWT* fly, its forehead is bulging, and its wings are partly unfurled.

The results of that retrospective analysis are plotted as histograms in Figure 8. The data confirm our preliminary suspicion that forelegs are somehow able to suppress t-row formation (induced by *Dll>ScrWT*) on their P surface more strongly than are midlegs: an average of only ~10 t-row bristles were typically elicited on the P side of basitarsi or tibias of forelegs, whereas twice that number was induced on the P side of basitarsi or tibias of midlegs. Likewise, the A/P ratio of t-row bristles averaged 5.6 for foreleg (basitarsi and tibias), but only 1.7 for midlegs (*vs*. 1.0 for *sca>ScrWT* in the present study) and 0.92 for hindlegs, respectively.

To solve this mystery it might help to recall a peculiar fact about midlegs: they express *Ubx* in their P half (Brower, 1987; Stern, 1998)—like hindlegs but more weakly (Held, 2002a). If (1) *Scr* does interact with *Ubx* as argued above, and (2) *en* can inhibit *Scr* on the P side of forelegs and midlegs, then the quantitative trends for *Dll>ScrWT* (Figure 8) are explicable as follows: (1) the *Dll-Gal4* driver can't raise *Scr* levels enough in the foreleg to overcome *en* inhibition, but (2) it is able—in combination with *Ubx*'s low background level—to double the number of t-row bristles on the P side of the midleg relative to the foreleg. Even with that *Ubx* boost, however, *Dll>ScrWT* can't surmount *en* inhibition all the way to an A/P ratio of 1.0—earning an A/P ratio of only 1.7 instead. So how does *sca>ScrWT* manage to attain a 1.0 ratio on the midleg while *Dll>ScrWT* falls short? Perhaps it fosters a higher level of *Scr* expression at later stages than *Dll>ScrWT*. These conjectures should be testable by (1) expressing *ScrWT* and *UbxWT* coordinately or (2) inducing *Ubx*-LOF or *en*-LOF clones in an *Scr*-GOF background.

Most of the extra t-row bristles that we found on *sca>ScrWT* midleg basitarsi abutted bristles within l-row 8 or row 1, rather than rows 7 or 2 (Figure 7). This affiliation of incipient t-rows with the ventral-most l-rows (8 and 1) suggests that t-rows on the foreleg and hindleg might normally develop similarly by adding bristle cells starting ventrally and spreading dorsally until they span the whole t-row area, instead of the other way around (*i.e*., dorsal to ventral).

Our finding that ectopic *Scr* can impose foreleg-specific traits (t-rows) on midlegs and hindlegs at a late (proneural cluster) stage agrees with the demonstrated ability of ectopic *Ubx* to induce hindleg traits (thin preapical bristle and stout tarsal bristle) in midlegs during bristle differentiation (Rozowski and Akam, 2002). In each case, bristle precursors can evidently be swayed by *Hox* influence to "change their minds" (leg identity) at the very last minute.

Expressing *ScrWT* via *Dll-Gal4* suppressed bracts on all six legs (Held, 2010), but expressing *ScrWT* by *sca-Gal4* deleted them to a variable extent on different leg segments. On *sca>ScrWT* forelegs, 57.9% (s.d. = 5.6; N = 10) of tibial bristles outside the t-row area lack bracts (*vs*. 7.4%; s.d. = 1.0; N = 10 in wild-type), whereas only 29.3% (s.d. = 6.4; N = 10) of bristles within the basitarsal t-row area lack them (*vs*. 0% in wild-type). The midleg tibia is missing bracts to a greater extent (70.4%; s.d. = 6.9; N = 10). We have conjectured

that high levels of Scr may be causing the bractless condition in the tibial t-rows of wild-type flies (Held, 2010), though it is hard to ascertain from published photos to what extent *Scr* is expressed more strongly on the tibia than on the basitarsus (Barmina and Kopp, 2007; Devi *et al.*, 2012; Randsholt and Santamaria, 2008; Shroff *et al.*, 2007; Tanaka *et al.*, 2011). For species that lack sex combs, such a bias (*i.e.*, higher on tibia) is indeed quite noticeable (A. Kopp, personal communication).

Many of these abnormalities were anticipated from our *Dll>ScrWT* study (Held, 2010), but one effect was a surprise (because our *Gal4* driver had been confined to legs): expression of *ScrWT* via *sca-Gal4* suppressed macrochaetes on the head and thorax (Figure 9). Macrochaetes are huge bristles that occupy constant positions from one fly to the next (Held, 2002a). Conceivably, *Scr* might impact them more than the smaller microchaetes, because their longer growth period (via polytenization) would prolong exposure to this "alien" transcription factor. Likewise, apical macrochaetes were missing from all *sca>ScrWT* midlegs (N = 20), and the big coxal bristles were shortened, but genuine signs of T2-to-T1 homeosis were also discernable: spur bristles at the apical site (Hannah-Alava, 1958) elongated to resemble tapered bristles of the foreleg's t-rows.

Conclusions

Hox genes are notorious for establishing "area codes" along the body axis in bilaterians (Held, 2017), and such broad "brush strokes" were probably their first major role in this clade. However, they also appear to have been recruited at various times for sundry "touch-up" chores (*cf.*, Stern, 1998 and 2003), and fly legs offer us a window into how such micro-managerial tasks are handled. Forelegs and hindlegs evolved peculiar rows of bristles (t-rows and sex comb) to serve adaptive needs aside from sensation—namely, grooming and grasping—and *Scr* and *Ubx* were somehow co-opted to implement the modular "subroutines" that govern those rows.

Whereas *Hox* genes encode segmental identity digitally as ON-OFF switches in embryos, *Scr* and *Ubx* seem to govern the later creation of t-rows and combs by an analog mode of action. The higher the dose of *Scr*, for example, the more t-rows arise on the foreleg tibia (Figure 5a), and *Scr* and *Ubx* appear to interact synergistically on the hindleg tibia (Figure 8a). Furthermore, the dosage of *Scr* may be instrumental in enforcing the bractless and yellowish state of t-row bristles on the tibia (*vs.*, the tarsus), though we still have no idea whether either of those tibia-specific traits are useful to the fly … or merely accidental side-effects of some obscure adaptive process.

Ultimately we would like to know how the t-rows and sex combs arose evolutionarily, how they are assembled developmentally, and how they are encoded genetically (Kopp, 2011). Answers to those questions might shed light on the genomic programming of bilaterian anatomy. Ever since Hanna-Alava mapped their intricacies in 1958, fly legs have offered a microcosm in which to explore deeper questions about patterning, and they continue to taunt us, despite all of the embarrassing situations we've contrived in an effort to pry from them their deepest secrets.

Acknowledgments: Fly stocks were obtained from Jeff Thomas (double-balancer strain, *y w; Sp/Cyo; Dr/TM3, Sb*, used to build our *sca-Gal4/CyO; Gal80^{ts}* stock) and from the Bloomington Stock Center: *sca-Gal4/CyO* (#42741), *neur-Gal4, Kg/TM3, Sb* (#6393), *UAS-dsScrRNAi* (B-50662), *UAS-ScrWT* (#7302), and *w; Sco/CyO; tub-Gal80^{ts}* (#7018). Critiques of the manuscript were provided by Markus Friedrich, Artyom Kopp, Nicolas Malagon, Marion Rozowski, Marc Srour, Kohtaro Tanaka, and Teresa Orenic, who helped resolve our A/P mystery. Zack Fitzgerald assisted in collecting virgins. This paper is dedicated to the memory of the Gerold Schubiger (1936-2012), who pioneered the use of fly legs as a model system 50 years ago (Beira and Paro, 2016; Schubiger, 1968). After receiving a diagnosis of the illness that would end his life, he contacted one of us (L.I.H.) to consult in the writing of his final paper on this topic—a masterpiece of Swiss precision (as usual). That paper, published in the year of his death (Schubiger *et al.*, 2012), inventoried all of the peculiar differences among the three pairs of legs.

References: Akam, M., 1998, Curr. Biol. 8: R676-R678; Ashburner, M., 1989, Drosophila: *A Laboratory Handbook*. CSH Press, N.Y.; Atallah, J., N.H. Liu, P. Dennis, A. Hon, D. Godt, and E.W. Larsen 2009, Evol. Dev. 11: 191-204; Atallah, J., G. Vurens, S. Mavong, A. Mutti, D. Hoang, and A. Kopp 2014, Dev. Biol. 386: 440-447; Barmina, O., and A. Kopp 2007, Dev. Biol. 311: 277-286; Beira, J.V., and R. Paro

2016, Chromosoma 125: 573-592; Belote, J.M., and B.S. Baker 1982, Proc. Natl. Acad. Sci. USA 79: 1568-1572; Brower, D.L., 1987, Development 101: 83-92; Casares, F., and R.S. Mann 2001, Science 293: 1477-1480; Castelli-Gair, J., and M. Akam 1995, Development 121: 2973-2982; Castro, B., S. Barolo, A.M. Bailey, and J.W. Posakony 2005, Development 132: 3333-3344; del Álamo, D., J. Terriente, and F.J. Díaz-Benjumea 2002, Development 129: 1975-1982; Devi, T.R., C. Amruthavalli, and B.V. Shymala 2012, Genesis 51: 97-109; Doe, C.Q., 2017, Annu. Rev. Cell Dev. Biol. 33: 219-240; Foronda, D., L.F. de Navas, D.L. Garaulet, and E. Sánchez-Herrero 2009, Int. J. Dev. Biol. 53: 1409-1419; García-Bellido, A., 1975, In: *Cell Patterning*. (Porter, R., and J. Rivers, eds.). Elsevier. 161-182; Hannah-Alava, A., 1958, J. Morph. 103: 281-310; Held, L.I., Jr., 1990, Roux's Arch. Dev. Biol. 199: 31-47; Held, L.I., Jr., 2002a, *Imaginal Discs: The Genetic and Cellular Logic of Pattern Formation*. Cambridge Univ. Press, New York; Held, L.I., Jr., 2002b, Mechs. Dev. 117: 225-234; Held, L.I., Jr., 2017, *Deep Homology?: Uncanny Similarities of Humans and Flies Uncovered by Evo-Devo*, Cambridge Univ. Press, New York; Held, L.I., Jr., 2010, Dros. Inf. Serv. 93: 132-146; Held, L.I., Jr., M.J. Grimson, and Z. Du 2004, Dros. Inf. Serv. 87: 76-78; Hurtado-Gonzales, J.L., W. Gallaher, A. Warner, and M. Polak 2015, Ethology 121: 45-56; Kopp, A., 2011, Evol. Dev. 13: 504-522; Lee, L.-W., and J.C. Gerhart 1973, Dev. Biol. 35: 62-82; Leung, B., and S. Waddell 2004, Trends Neurosci. 27: 511-513; Malagon, N., and E. Larsen 2015, Int. Rev. Cell Mol. Biol. 315: 153-181; McGuire, S.E., G. Roman, and R.L. Davis 2004, Trends Genet. 20: 384-391; Mlodzik, M., N.E. Baker, and G.M. Rubin 1990, Genes Dev. 4: 1848-1861; Nottebohm, E., A. Usui, S. Therianos, K.-I. Kimura, C. Dambly-Chaudière, and A. Ghysen 1994, Neuron 12: 25-34; Pavlopoulos, A., and M. Akam 2011, PNAS 108, #7: 2855-2860; Randsholt, N.B., and P. Santamaria 2008, Evol. Dev. 10: 121-133; Renaud, O., and P. Simpson 2001, Dev. Biol. 240: 361-376; Rozowski, M., and M. Akam 2002, Genes Dev. 16: 1150-1162; Schubiger, G., 1968, W. Roux' Arch. Entw.-Mech. Org. 160: 9-40; Schubiger, G., M. Schubiger, and A. Sustar 2012, Dev. Biol. 369: 76-90; Shroff, S., M. Joshi, and T.V. Orenic 2007, Mechs. Dev. 124: 43-58; Stern, D.L., 1998, Nature 396: 463-466; Stern, D.L., 2003, Dev. Biol. 256: 355-366; Struhl, G., 1982, Proc. Natl. Acad. Sci. USA 79: 7380-7384; Szebenyi, A.L., 1969, Anim. Behav. 17: 641-651; Tanaka, K., O. Barmina, L.E. Sanders, M.N. Arbeitman, and A. Kopp 2011, PLoS Biol. 9, #8: e1001131; Troost, T., M. Schneider, and T. Klein 2015, PLoS Genet. 11, #1: e1004911; Tsubota, T., K. Saigo, and T. Kojima 2008, Mechs. Dev. 125: 894-905; Vandervorst, P., and A. Ghysen 1980, Nature 286: 65-67; Yeh, E., L. Zhou, N. Rudzik, and G.L. Boulianne 2000, EMBO J. 19: 4827-4837.

Enhancer of *dumpy-vortex* [*e*(*dp*^{v})] also enhances *dumpy-oblique* (*dp*^{ov1}).

Thompson, Steven, and Ross MacIntyre. Molecular Biology and Genetics, Cornell University and Ithaca College, Ithaca, New York 14853. Corresponding Author: Ross MacIntyre; email address: rjm18@cornell.edu.

The complex *dumpy* gene (Wilkin *et al*., 2000) is an important component of the extracellular matrix of epithelial cells throughout development. *Dumpy* mutants fall into three classes, those that affect wing shape (oblique mutants), those that affect tendon cell attachment to the adult dorsal thoracic cuticle (vortex mutants), and those that affect viability (lethal mutants). Single mutants can affect one, two, or all three of these phenotypes. Following Grace *et al*. (1980), we have developed a scoring system for the oblique phenotype (Carmon *et al*., 2010). Wild type wings are scored as zero, whereas dumpy mutant wings are scored from one to five with five indicating the most severe truncation and/or distorted wing shape.

As part of our ongoing study of dumpy's interactions with other genes, we have examined the extent of the interaction between dumpy mutants and a gene discovered about 100 years ago by Calvin Bridges (Bridges and Mohr, 1919) originally called "enhancer of dumpy vortex" and now designated as *e*(*dp*^{v}) in flybase. We made double mutant combinations of *e*(*dp*^{v}) and the canonical dumpy oblique mutant, *dpy*^{ov1}, which shows an intermediate expression of the oblique phenotype but variable expression of dumpy vortex. Our results, using the scoring system described above are shown in the table below: